Electronic Supplementary Information **(ESI)**

In vitro and environmental toxicity of reduced graphene oxide as an additive in automotive lubricants

Margarita Esquivel-Gaon[a§], Nhung H. A. Nguyen[b§], Mauro F. Sgroi[c], Daniele Pullini[c], Flavia Gili[c], Davide Mangherini[c], Alina Iuliana Pruna[d,e], Petra Rosicka[b], Alena Sevcu[b] and Valentina Castagnola[a*]

[a.] *Centre for BioNano Interactions, School of Chemistry and Chemical Biology, University College Dublin, Belfield, Dublin 4, Dublin, Ireland.*

[b.] *Technical University of Liberec, Institute for Nanomaterials, Advanced Technologies and Innovation, Bendlova 1409/7 CZ-461 17 Liberec*

[c.] *Centro Ricerche FIAT, Strada Torino 50, 10043 Orbassano (TO), Italy*

[d.] *Gemmate Technologie, via Reano 31, 10090 Buttigliera Alta (TO), Italy*

[e.] *Center for Surface Science and Nanotechnology, Polytechnic University of Bucharest, 313 Splaiul Independentei, 060042 Bucharest, Romania.*

§ These authors contributed equally to this work

* Corresponding Authors

Table of Contents

1 Synthesis and characterisation of rGO (Gemmate Technologies)

1.1 Synthesis of rGO

The chemically reduced graphene oxide (rGO or CrGO) nanomaterial (Gemmate Technologies) was obtained by using a modified Hummers method[1] in which graphite powder was oxidized with H_2SO_4 and $KMnO_4$. The obtained GO was purified with HCl, washed to neutral pH and dried at 50 °C for 24 h. For the chemical conversion of GO into rGO, ascorbic acid was added (10:1 w/w ascorbic acid:GO) to an aqueous dispersion of GO (0.5 mg/mL). The reduction took place under mechanical stirring at room temperature for 6 h.

1.2 Characterization of rGO

1.2.1 Transmission Electron Microscopy (TEM)

TEM images of both GO and rGO were acquired using a JEM-1010 (JEOL) microscope.

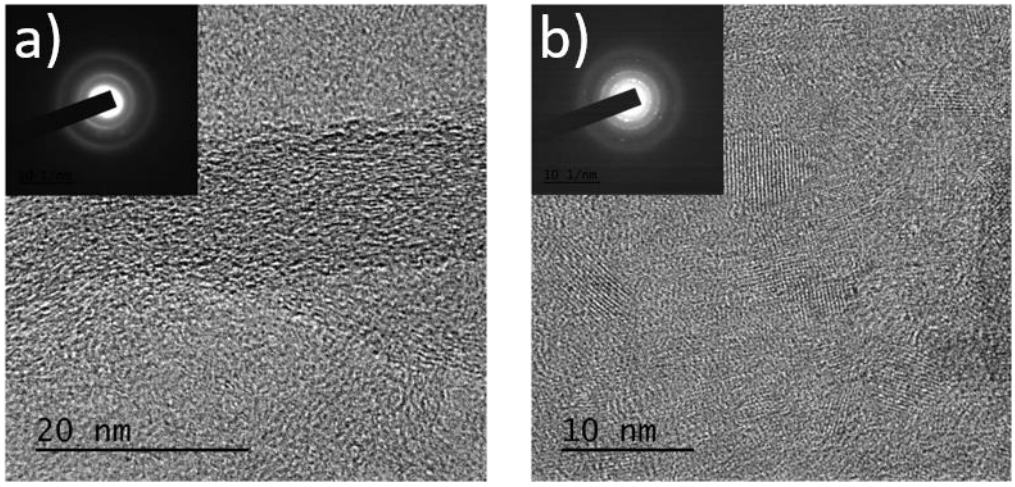

Figure S-1. TEM images for GO (a) and rGO (b) and insets with selected area diffraction patterns (SAED).

Folding and wrinkling phenomena were observed for both GO and rGO. The edges present a few-layered structure such as mono-, double- or multi-layers. With respect to the amorphous GO, the partial removal of oxygen functional groups in CrGO by wet chemistry resulted in a material with crystalline fragments (see insets).

1.2.2 X-ray diffraction (XRD)

The XRD measurements were performed on a D2 Phaser (Bruker) diffractometer using Cu-Ka radiation and 30 kV voltage. The acquired spectra depicted in fig. S2 show the effects of oxidation and reduction processes on typical (002) diffraction peak of graphite towards formation of GO and rGO.

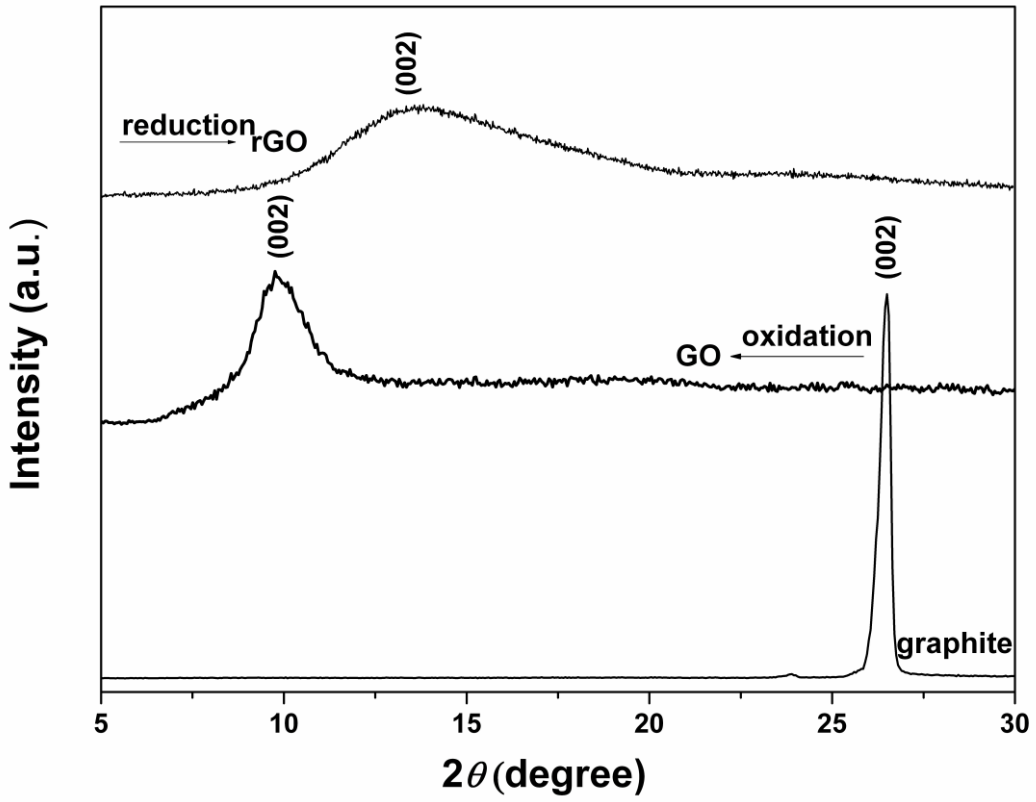

Figure S-2. XRD spectra for GO and rGO.

The XRD spectrum of graphite showed a sharp intense (002) peak at about 26.5 deg. while the introduction of oxygen groups during oxidation procedure shifted such peak towards 9.2 deg. Upon chemical reduction, the rGO showed a crystal structure with a much smaller interlayer spacing with respect to GO as demonstrated by the full width half maximum values in Fig. S-2, due to the removal of functional groups between the layers. The arrows in the image illustrate the evolution of (002) diffraction peak upon chemical introduction and removal of oxygen groups in GO and rGO, respectively.

1.2.3 Thermogravimetric Analysis (TgA)

TGA was performed on a Q50 analyzer (TA Instruments) using a scanning rate of 10 K min –1 under N2 flow. The TGA curves in Fig. S-3 show a variable content of oxgyen functionalities in GO with three weight step loses.

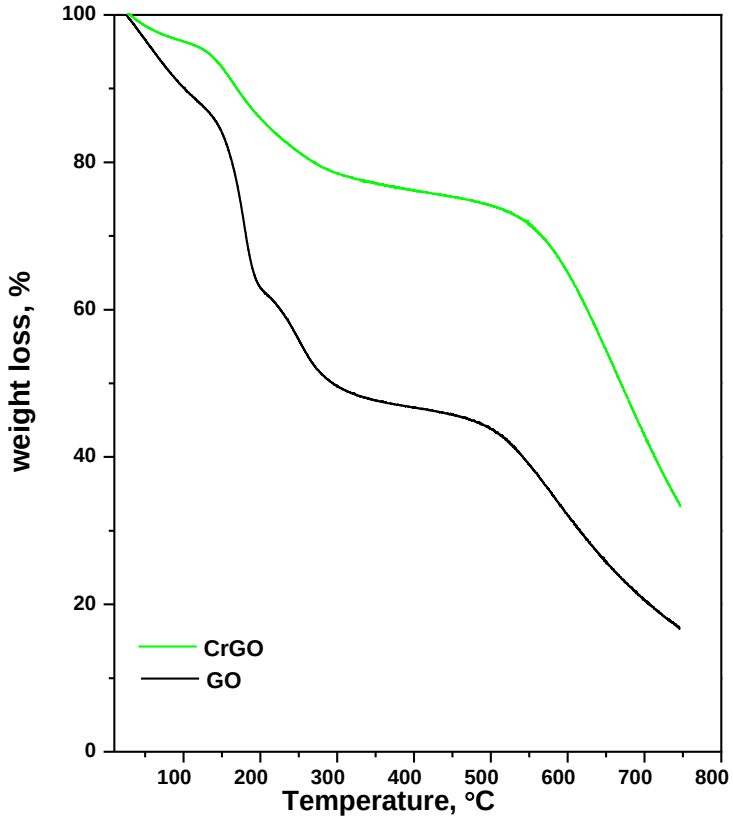

Figure S-3. TGA weight loss showing thermal stability of rGO (green) in comparison with GO (black).

A partial removal of oxygen groups in GO was observed upon the chemical reduction: following the initial weight loss of about 15 % at 100 °C (and about 5% in case of rGO) ascribed to the removal of loosely bound or adsorbed water and gas molecules, the labile oxygen-containing functional groups are pyrolized up to 600 °C followed by the more stable ones, yielding CO, CO_2, and steam. The thermal beaviour of rGO shows greater stability with respect to GO due to the partial removal of functional groups.

1.2.4 Raman spectroscopy

A strong G band around 1595 cm^{-1} related to the vibration of sp^2-bonded carbon atoms and a weak D band around 1350 cm^{-1} associated with structural imperfections of graphene sheet and disorders were exhibited by the spectra of GO and CrGO in figure 5. The shifts in the band positions and their intensity evolution indicate a partial removal of the functional groups in rGO together with an increased level of defects, as demonstrated by the increased I_D/I_G ratio from 0.73 in GO to 1.28 in rGO.

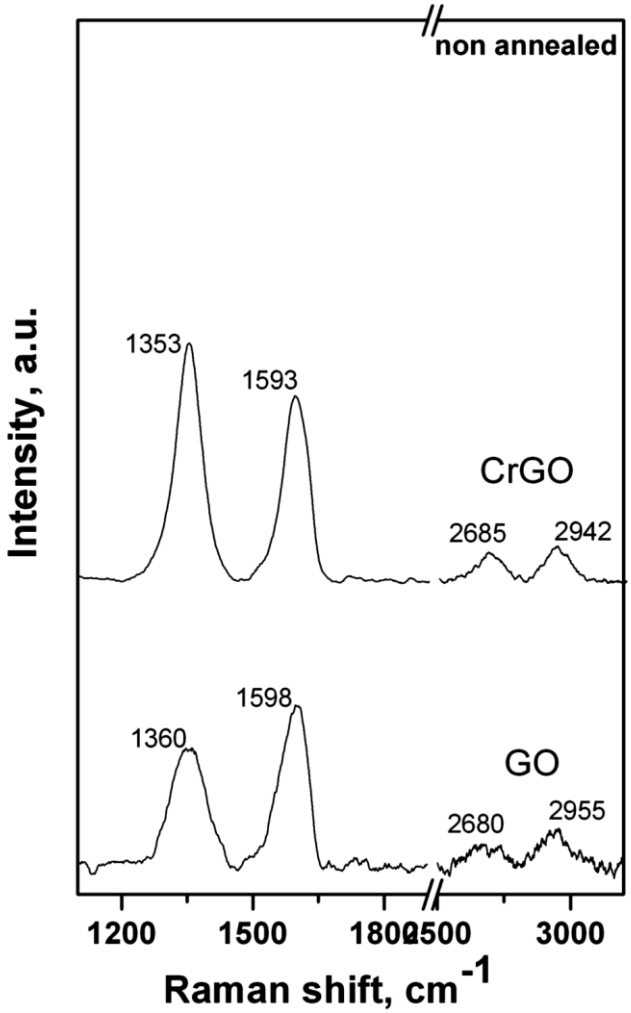

Figure S-4. Raman spectra for GO and rGO.

1.2.5 X-ray photoelectron spectroscopy

X-ray photoelectron spectroscopy (XPS) analysis was performed on an Omicron spectrometer system using Mg-K a radiation (1253.6 eV). Survey scan spectra were obtained at 50 eV pass energy, while individual high resolution spectra were recorded at 20 eV pass energy. The binding energies were referenced to the C1s line at 284.6 eV.

The peak areas calculation of C and O elements from XPS spectra survey scan in figure 6 revealed that the C/O atomic ratio increased from 2.8 in GO to 7.14 in rGO. The C1s band was fitted to six components: (1) located at the binding energy of at 284.44 eV (C=C species), (2) and (3) located at 285.36 eV and 286.94 eV (assigned them to C–OH and epoxy C–O groups), (4) at 287.75 eV (>C=O), (5) at 288.52 (COOH) and (6) at 289.04 eV (shake-up satellite band of graphitic carbon band).

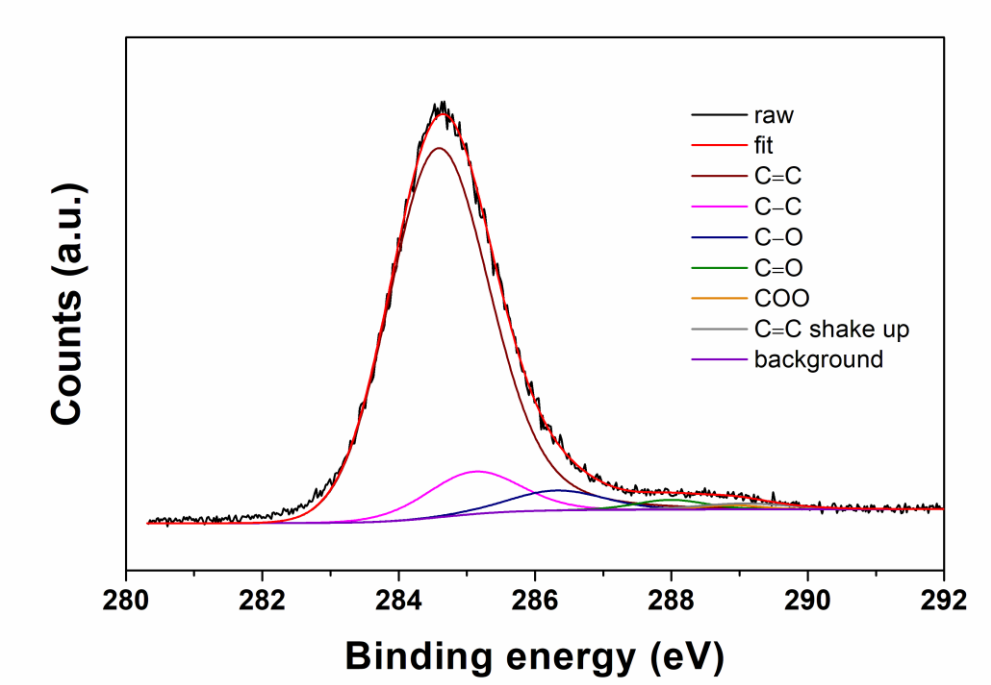

Figure S-5. High resolution C1s XPS spectra deconvoluted peaks for rGO materials.

2 Biological aqueous dispersion of rGO (G-aq)

rGO samples have been dispersed in water by mean of complete foetal bovine serum (FBS) under ultrasonication. A starting concentration of 10 mg/mL rGO was dispersed in a solution of 50% v/v FBS in Phosphate Buffered Saline (PBS) and sonicated for 1h with tip sonicator. The undispersed flakes are discarded by centrifugation at 1500 rpm for 15 min and only the supernatant was kept for the washing phase. From the supernatant, different fraction could be separated by centrifugation steps at increasing speed.

The excess of proteins was then washed by three sub sequential centrifugations at maximum speed (14000 rpm) for 20 min, and the supernatant was discarded each time and replaced with fresh PBS.

2.1 Differential centrifugal sedimentation (DCS) analysis

Differential Centrifugal Sedimentation (DCS) analysis cannot be considered to give a formally correct size distribution in the case of non-spherical particles. However, it can produce very consistent and repeatable results even applied to graphene,[2] and allows to distinguish different populations and to detect aggregation. Here, the DCS distribution of two rGO dispersions in water (SG-aq and LG-aq) is reported in Figure S-6.a. DCS have been also employed to check the stability of rGO dispersion in bacterial growth media and the results are reported in Figure S-6.b.

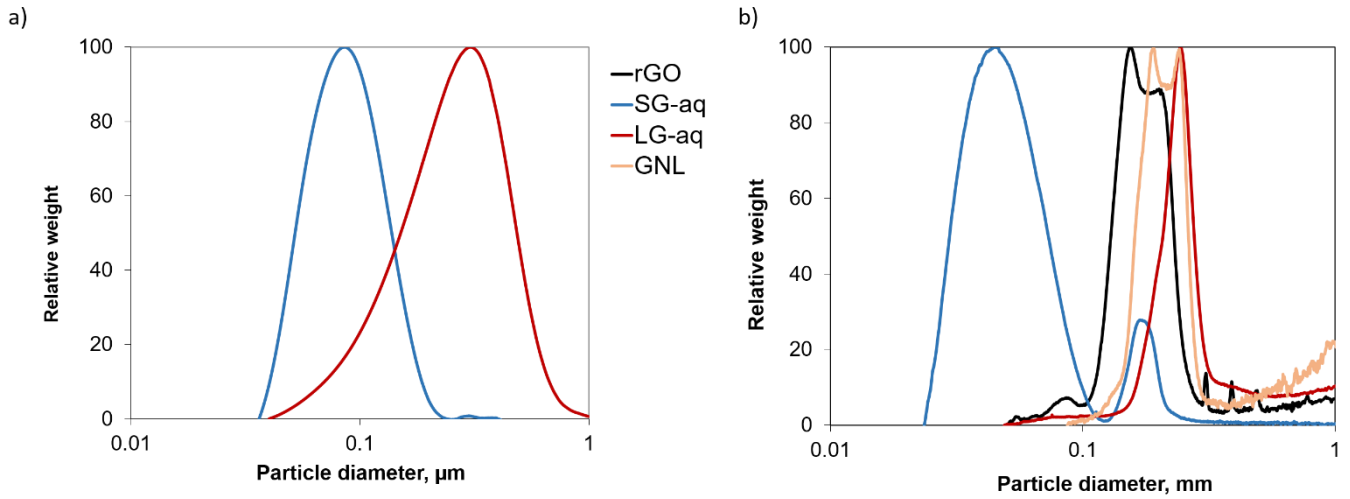

Figure S-6. DCS analysis for a) small and large population of rGO nanosheets in aqueous suspension (SG-aq and LG-aq) after sonication with full serum and b) SG-aq, LG-aq, rGO and GNL (rGO in base oil) after dispersion in bacterial growth media.

As expected, the water dispersions SG-aq and LG-aq showed a better stability in bacterial growth media compared to the lubricant (GNL) and rGO powder sonicated for 30 min in deionized water.

3 *In vitro* cell toxicity

3.1 LG-aq uptake: TEM imaging

TEM images on cells slices validate the uptake evaluation by flow cytometry, showing that the graphene nanosheets are actually internalised by the cells.

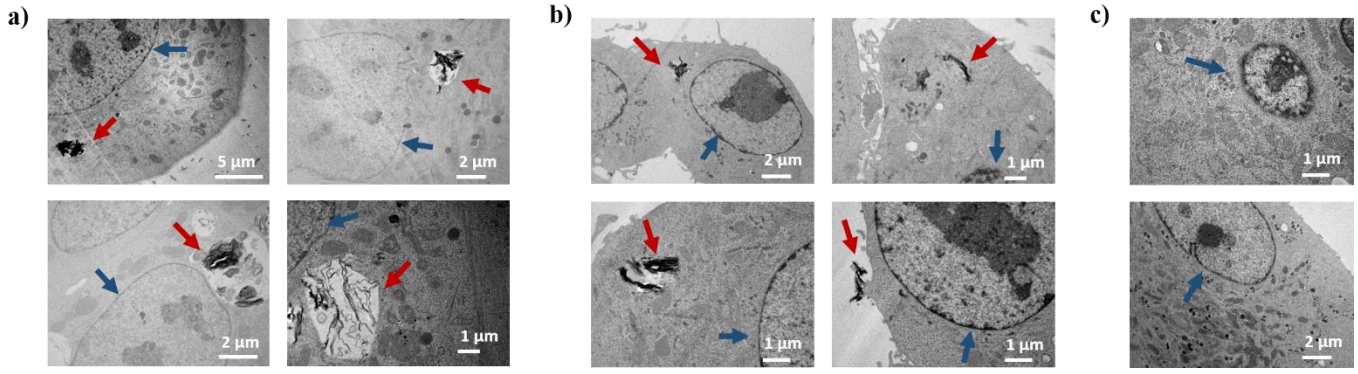

Figure S-7. TEM images of a) A549, b) RAW264.7 cell slices after incubation with 50 µg/ml of LG-aq for 7h. Red arrows indicate LG-aq material inside the cell cytoplasm and blue arrows indicate the cell nucleus. c) A549 cell control (not exposed to LG-aq).

3.2 Cell Viability

The mitochondrial activity was evaluated by using the CellTiter 96 Aqueous One Solution Assay (Promega). The bioreduction of 3-(4,5-dimethylthiazol-2-yl)-5-(3-carboxymethoxyphenyl)-2-(4-sulfophenyl)-2H-tetrazolium, inner salt (MTS) and an electron coupling reagent (phenazine ethosulfate; PES) by healthy cells in to a formazan soluble product that can be quantify by measuring the absorbance at 490 nm; the results are directly proportional with metabolically active cells / mitochondrial activity and live cells in proliferation. It is well accepted for graphene and other carbon-based nanomaterials that MTT assay is not suitable for evaluating the cells viability due to the commonly occurring false positive.[3] Although WST-8 is considered the most reliable methods, several works in the literature demonstrate that the results obtained by WST-8 are comparable to that obtained by MTS assay,[4-6] thus validating the method that was therefore employed in this work.

A549 and RAW 264.7 cells were seeded in 96 well plates, and after 24 hours LG-aq was added in increasing concentrations and cell were further incubated for 24 and 72 hours, and then 10 µL of the Aqueous One Solution reagent was directly added to the cells in culture. After 1 hour incubation, the absorbance was measured with a microplate reader (Varioskan Flash, Thermo Fisher). Each experiment was done in triplicate and repeated at least twice. The mitochondrial activity (%) is related to control wells without treatment.

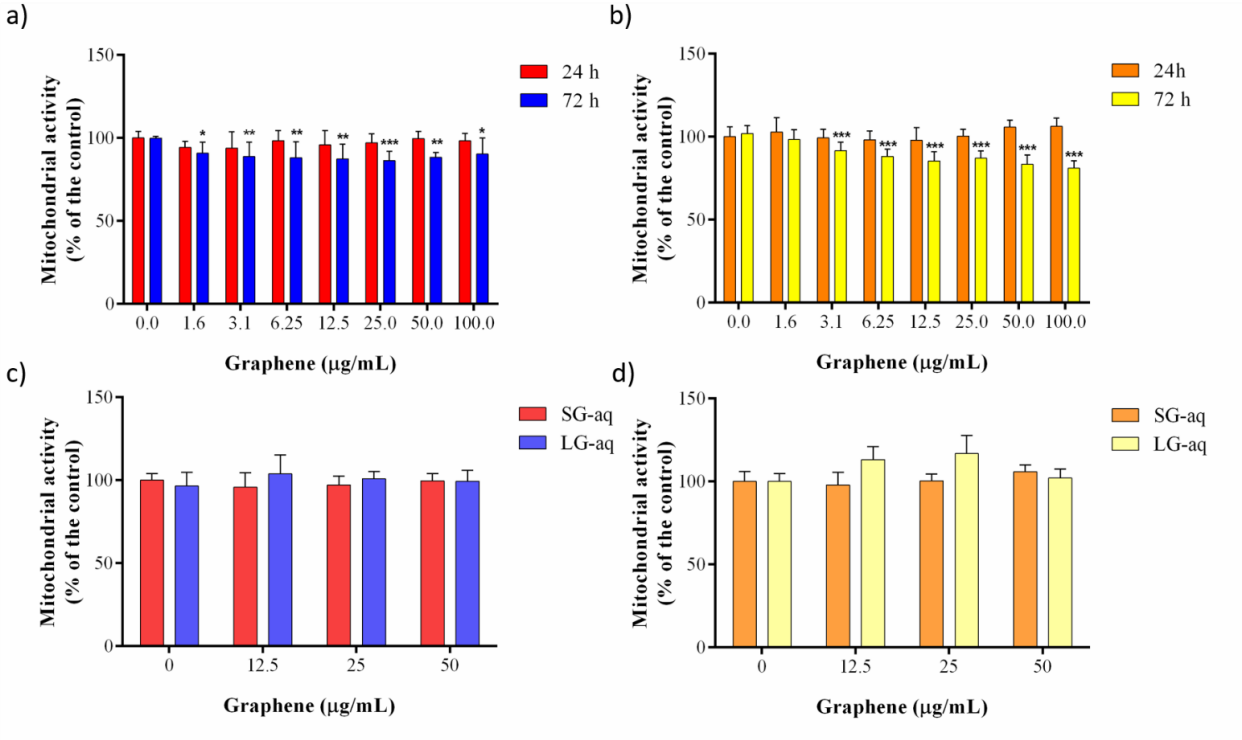

Figure S-8. Cell viability measured by the mitochondrial activity after the exposure to biological dispersion of rGO. a) A549 and b) Raw 264.7 cells were exposed to different concentrations of SG-aq for 24h and 72h. c) A549 and d) Raw 264.7 cells exposed to different concentrations of both LG-aq and SG-aq for 24h. Graphs represent the mean ± SD derived from two independent experiments, assayed in triplicate. Statistical significance was determined using a two-way ANOVA and Dunnett's comparison test vs. the control (0 µg/mL); *p <0.05, **p<0.01; ***p<0.001. LG-aq and SG-aq when compared presented no significant differences.

3.3 High Content Analysis: merged epifluorescence images

High Content Analysis (HCA) approach was used to evaluate cellular cytotoxicity and lysosomal activity. A549 and RAW 264.7 cells were seeded in 96 well plates and after 24 hours LG-aq were added at a final concentration of 25, 50, 100 and 200 µg/mL and cells were further incubated for 24 hours. The dyes were added to the cell culture after the end of the incubation period, the dyes used were the following: Hoechst (400 nM), Lysotracker red (200nM) and TOPRO-3 (800nM). After 1 hour of incubation cells were analysed by High Content Analysis using the Arrayscan VTI 740 (Thermo Scientific). Images were acquired using a 20x objective and fluorescence emission was collected using a combination of excitation/emission filters appropriated for the dyes used. Each experiment was done in triplicate and repeated at least twice. The fluorescence intensity of each dye was compared to control wells without treatment.[7]

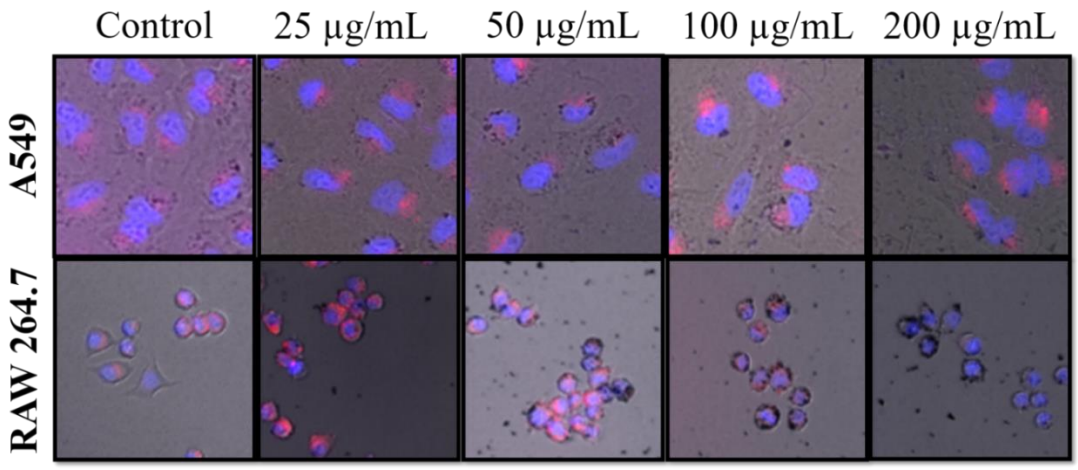

Figure S-9. Epifluorescence representative images of A549 and RAW 264.7 cells exposed to SG-aq nanoparticles for 24 h. Live cells nuclei (blue), Lysosomes (red), dead cells nuclei (purple).

4 Environmental toxicity

4.1 Bacterial morphology imaged by Scanning Electron Microscopy (SEM)

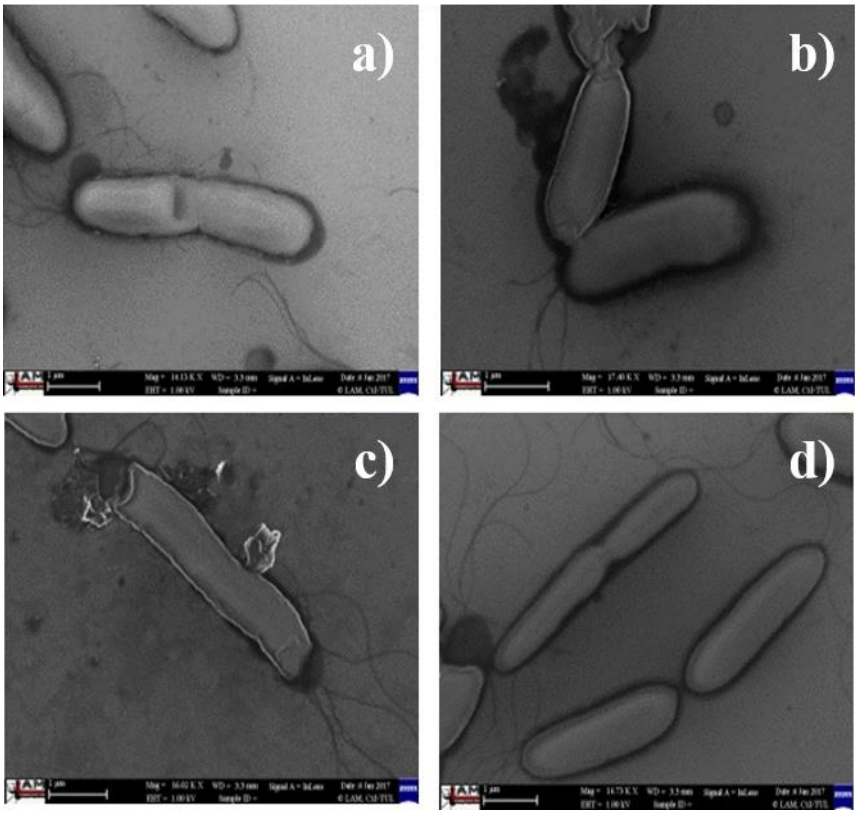

Figure S-10. Morphology of bacterial cells incubated with A) Control, B) rGO, C) SG-aq and D) LG-aq for 24h. Scale bar is 1 µm.

4.2 DNA fragmentation

The cells were incubated with GNL, pristine rGO, SG-aq and LG-aq (all 100 µg/mL final. conc.) and control cells without rGO for 24 h. Then the cells were lysed in 250 µL of cell lysis buffer containing 50 mM of Tris-HCl, 10 mM ethylenediaminetetraacetic acid, 0.1 M NaCl, 0.5% SDS, and pH 8.0. The lysate was incubated with 0.5 mg/mL RNase A at 37 °C for 1 h, and then with 0.2 mg/mL proteinase K at 50 °C overnight. Phenol extraction of this mixture was performed, and DNA in the aqueous phase was precipitated by using 25 mL (1/10 vol) of 7.5 M ammonium acetate and 250 mL (1/1 vol) of isopropanol. DNA electrophoresis was performed in 1% agarose gel containing 1 mg/mL of ethidium bromide at 70 V, and the DNA fragments were visualized by exposing the gel to UV light, followed by photography.[8]

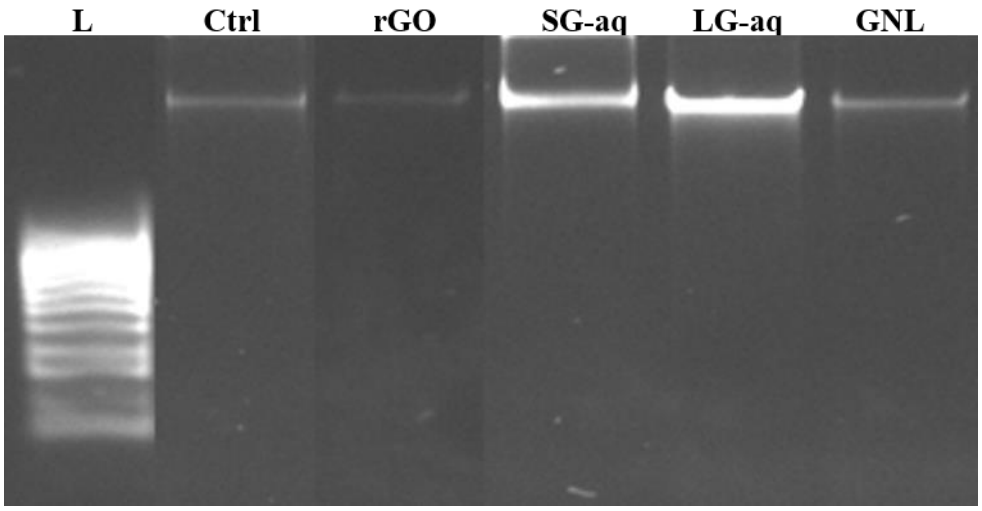

Figure S-11. DNA fragmentation of bacterial growth with different rGO suspensions after 24h. The lanes are in the order: DNA marker (L), Control (Ctrl) (*P. putida* without rGO), pristine rGO, SG-aq, LG-aq and GNL.

5 References

1. W. S. Hummers Jr and R. E. Offeman, *Journal of the American Chemical Society*, 1958, **80**, 1339-1339.
2. R. Wang, Y. Ji, X. Wu, R. Liu, L. Chen and G. Ge, *RSC Advances*, 2016, **6**, 43496-43500.
3. K.-H. Liao, Y.-S. Lin, C. W. Macosko and C. L. Haynes, *ACS applied materials & interfaces*, 2011, **3**, 2607-2615.
4. V. Gies and S. Zou, *Toxicology Research*, 2018.
5. C. M. Santos, J. Mangadlao, F. Ahmed, A. Leon, R. C. Advincula and D. F. Rodrigues, *Nanotechnology*, 2012, **23**, 395101.
6. S. Makharza, G. Cirillo, A. Bachmatiuk, I. Ibrahim, N. Ioannides, B. Trzebicka, S. Hampel and M. H. Rümmeli, *Journal of nanoparticle research*, 2013, **15**, 2099.
7. S. Anguissola, D. Garry, A. Salvati, P. J. O'Brien and K. A. Dawson, *PloS one*, 2014, **9**, e108025.
8. S. Gurunathan, J. W. Han, A. A. Dayem, V. Eppakayala and J.-H. Kim, *International journal of nanomedicine*, 2012, **7**, 5901.